Cell lines

All cell lines were obtained from the American Type Culture Collection. Cultures were grown in aseptic conditions at 37 ºC and 5% CO_2 in a humidified atmosphere. NCI-H660 cells were grown in DMEM/F12 medium supplemented with 10% fetal bovine serum, 10 nM beta-estradiol, 10 nM hydrocortisone, 30 nM sodium selenite, 0.005 mg/mL insulin, 0.01 mg/mL transferrin, 4 mM L-glutamine, 100 units/mL penicillin, and 100 µg/mL streptomycin. DU145 cells were grown in DMEM medium supplemented with 10% fetal bovine serum, 100 units/mL penicillin, and 100 µg/mL streptomycin. LNCaP cells were grown in RPMI-1640 medium supplemented with 10% fetal bovine serum, 100 units/mL penicillin, and 100 µg/mL streptomycin. H82 cells were cultured in RPMI-1640 medium supplemented with 10% fetal bovine serum, 2 mM L-glutamine, 10 mM HEPES, 1 mM sodium pyruvate, 4.5 g/L glucose, 1.5 g/L sodium bicarbonate, 100 units/mL penicillin, and 100 µg/mL streptomycin. PC3 cells were grown in F-12 Kaighn's medium supplemented with 10% fetal bovine serum, 100 units/mL penicillin, and 100 µg/mL streptomycin.

RNA isolation and quantitative real-time PCR

Approximately 5 million cells were pelleted and washed with PBS before proceeding to RNA extraction. RNA extraction from cell pellets was done using RNeasy mini kit (QIAGEN). On column DNA digestion was done using RNase-Free DNase set (QIAGEN). RNA quality and quantity were determined using a spectrophotometer at 260 and 280 nm (Nanodrop-2000, Thermo Scientific). cDNA was generated using the High Capacity cDNA Reverse Transcription Kit (Applied Biosystems; Life Technologies). Quantitative-PCR was performed using RT^2 SYBR Green Fluor qPCR Mastermix and RT^2 qPCR primers (Qiagen) on a CFX96 Touch Real-

Time PCR Detection System (Bio Rad). *DLL3*, *ASCL1*, *SOX2*, *AR*, *FOLH1 (PSMA)*, and *KLK3 (PSA)* expression were quantified relative to beta actin using the comparative CT method. Log_2 fold changes were calculated by comparing expression levels to negative control H82 and A549 human lung cancer cell lines.

Synthesis of ^{89}Zr-DFO-SC16

The DFO-SC16 (or DFO-IgG control) was produced by the incubation of SC16 with a 6-molar excess of the chelator *p*-isothiocyanatobenzoyl desferrioxamine (*p*-SCN-DFO, Macrocyclics, Inc.) at a pH of 9 and 25 ºC for 90 min on a thermomixer. The immunoconjugates were purified by size exclusion chromatography on a PD-10 desalting column (GE Healthcare) and concentrated with a 50,000 MWCO Amicon centrifugal filter. Zirconium-89 (^{89}Zr) was produced by the proton bombardment of ^{89}Y foil on a cyclotron and supplied by the Radiochemistry & Molecular Imaging Probes core at Memorial Sloan Kettering Cancer Center. The ^{89}Zr-oxalate solution (5.55 MBq) was adjusted to pH 6.5–7.0 by addition of 1 M sodium carbonate (Na_2CO_3) and incubated at room temperature with the DFO-mAbs (15 μg) for 1 hour on a thermomixer. The ^{89}Zr-DFO-mAbs were purified on a PD-10 desalting column and radiochemical purity was assessed by radio-instant thin layer chromatography (radio-iTLC) using 50 mM ethylenediaminetetraacetic acid (EDTA) as the eluent. The radioimmunoconjugate stability and demetallation of ^{89}Zr was evaluated in an *in vitro* serum stability assay by incubating ^{89}Zr-DFO-SC16 in human serum at 37 ºC for 5 days. Radiochemical purity and demetallation of ^{89}Zr were determined via radio-iTLC.

In vitro bead-based binding assay

To determine the DLL3 target-binding fraction of ^{89}Zr-DFO-SC16, a bead-based radioligand binding assay was performed using magnetic beads functionalized with His-tagged DLL3 protein (R&D Systems). For the control, the procedure was the same except no His-tagged DLL3 was added to assess non-specific binding of ^{89}Zr-DFO-SC16 to the magnetic beads alone. For the block, the procedure was the same except 5 μg of DFO-SC16 was also added to determine specificity of ^{89}Zr-DFO-SC16 binding to His-tagged DLL3.

In vitro saturation binding assay

A 0.15 μg/mL solution of ^{89}Zr-DFO-SC16 was prepared in PBS with 1% BSA. 3 ng (20 μL) of the radiolabeled construct was added to an Eppendorf tube containing $10x10^6$ cells in 0.2 mL of culture media. The mixture was allowed to incubate for 1 hour with intermittent pipetting up/down every 15 minutes to resuspend the cells. Next, the cells were centrifuged (600 x g for 5 min) followed by pipetting out the media supernatant to another centrifuge tube. Then, the cells were washed with 1 mL of ice-cold PBS, centrifuged (600 x g for 5 min), and the PBS supernatant was pipetted out into a separate Eppendorf tube. The washing procedure was repeated two more times. Lastly, the cell pellet, the media supernatant, and the three wash fractions were placed on a gamma counter to determine the percent of cell bound radioactivity of the radiolabeled construct. The above procedure was repeated for a 0.15 μg/mL solution of ^{89}Zr-DFO-IgG in PBS with 1% BSA.

Immunohistochemistry

The immunohistochemistry detection of AR, DLL3, Synaptophysin, and PSMA were performed at Molecular Cytology Core Facility of Memorial Sloan Kettering Cancer Center, using

Discovery XT processor (Ventana Medical Systems, Roche - AZ). After 32 min of heat and CC1 (Cell Conditioning 1, Ventana catalog#: 950-500) retrieval, the tissue sections were blocked first for 30 min in Background Blocking reagent (Innovex, catalog#: NB306).

A rabbit monoclonal anti-AR antibody (Epitomics, catalog#: 3184-1) was used in 0.66 µg/mL concentration. The incubation with the primary antibody was done for 5 h, followed by 60 min incubation with biotinylated goat anti-rabbit IgG (Vector labs, catalog#: PK6101) in 5.75 µg/mL. Blocker D, Streptavidin- HRP and DAB detection kit (Ventana Medical Systems) were used according to the manufacturer instructions. The slides were counterstained with hematoxylin and coverslipped with Permount (Fisher Scientific).

A rabbit monoclonal anti-DLL3 antibody (Ventana Ref#: 790-7016) was used in prediluted ready to use concentration. The incubation with the primary antibody was done for 4 h, followed by 60 min incubation with biotinylated goat anti-rabbit IgG (Vector labs, catalog#: PK6101) in 5.75 µg/mL, followed by application of Blocker D, Streptavidin- HRP and DAB detection kit (Ventana Medical Systems), according to the manufacturer instructions. The slides were counterstained with hematoxylin and coverslipped with Permount (Fisher Scientific).

A rabbit monoclonal anti-Synaptophysin antibody (Epitomics, catalog#: 1485) was used in 0.05 µg/mL concentration. The incubation with the primary antibody was done for 6 h, followed by 60 min with biotinylated goat anti-rabbit IgG (Vector labs, catalog#: PK6101) in 5.75 µg/mL. Blocker D, Streptavidin- HRP and DAB detection kit (Ventana Medical Systems) were used according to the manufacturer instructions. The slides were counterstained with hematoxylin and coverslipped with Permount (Fisher Scientific).

A rabbit polyclonal anti-PSMA antibody (Proteintech, catalog#: 13163-1-AP) was used in 1 µg/mL concentration. The incubation with the primary antibody was done for 5 h, followed

by 60 min incubation with biotinylated goat anti-rabbit IgG (Vector labs, catalog#: PK6101) in 5.75 µg/mL. Blocker D, Streptavidin- HRP and DAB detection kit (Ventana Medical Systems) were used according to the manufacturer instructions. The slides were counterstained with hematoxylin and coverslipped with Permount (Fisher Scientific).

Subcutaneous xenograft model

To develop the subcutaneous xenograft models, 6–8-week-old male athymic nude mice were injected subcutaneously on the left shoulder with 5 million H660 cells or DU145 cells in 1:1 media/matrigel basement membrane matrix (BD Biosciences). To generate the dual subcutaneous xenograft model, 6-8 week old male athymic nude mice were injected with 5 million H660 cells subcutaneously on the left shoulder and with 5 million LNCaP cells on the right shoulder in 1:1 media/matrigel basement membrane matrix. The tumors were allowed to grow for 3–5 weeks, and then the mice were used for PET imaging and biodistribution studies.

Biodistribution Studies

For biodistribution studies, mice were warmed under a heat lamp prior to administration of the radioimmunoconjugates (1.00–3.80 MBq; 2.7–10.3 µg in 200 µL chelexed PBS for H660 tumors) (0.32–0.98 MBq; 0.87–2.7 µg in 200 µL chelexed PBS for DU145 tumors) via intravenous tail vein injection (t = 0). Mice were euthanized by CO_2 asphyxiation at 24, 72, and 120 h post tracer administration. For the blocking study, a co-injection of ^{89}Zr-DFO-SC16 (0.94–0.97 MBq; 2.55–2.63 µg in 200 µL chelexed PBS) and 50-fold excess of cold, unlabeled SC16 was injected into the mice and then euthanized at 72 h post-injection. Non-specific uptake in DLL3-positive H660 subcutaneous xenografts was determined by injection with ^{89}Zr-DFO-IgG

(3.60-3.70 MBq; 9.7–10.0 μg in 150 μL chelexed PBS) and then euthanized at 120 h post-injection. After asphyxiation, organs of interest and the tumor were harvested, weighed, and counted on a gamma-counter to determine accumulation of radioactivity. The mass of the injected radioimmunoconjugates were measured and compared to a standard syringe of known activity and mass to determine the total number of counts injected per mouse. The percent injected dose per gram (%ID/g) was determined for each sample by normalizing the counts per sample to the total amount of activity injected.

PET/CT Imaging

Mice bearing H660 subcutaneous tumors were intravenously injected with ^{89}Zr-DFO-SC16 (3.60–3.80 MBq; 9.7–10.3 μg in 150 μL chelexed PBS) or ^{89}Zr-DFO-IgG (3.60–3.70 MBq; 9.7–10.0 μg in 150 μL chelexed PBS) or ^{68}Ga-DOTATATE (7.66–8.33 MBq in 150 μL formic acid, sodium hydroxide, and sterile water solution). Mice bearing DU145 subcutaneous tumors were intravenously injected with ^{89}Zr-DFO-SC16 (5.85–6.22 MBq; 15.8–16.8 μg in 150 μL chelexed PBS). Mice bearing dual LNCaP and H660 tumors were intravenously injected with ^{89}Zr-DFO-SC16 (4.42–4.62 MBq; 11.9–12.5 μg in 150 μL chelexed PBS) and ^{68}Ga-PSMA-11 (8.66–8.92 MBq in 150 μL sterile acetate buffer). Mice were anesthetized with 1–2% isoflurane and images were acquired from an Inveon microPET/CT instrument (Siemens).

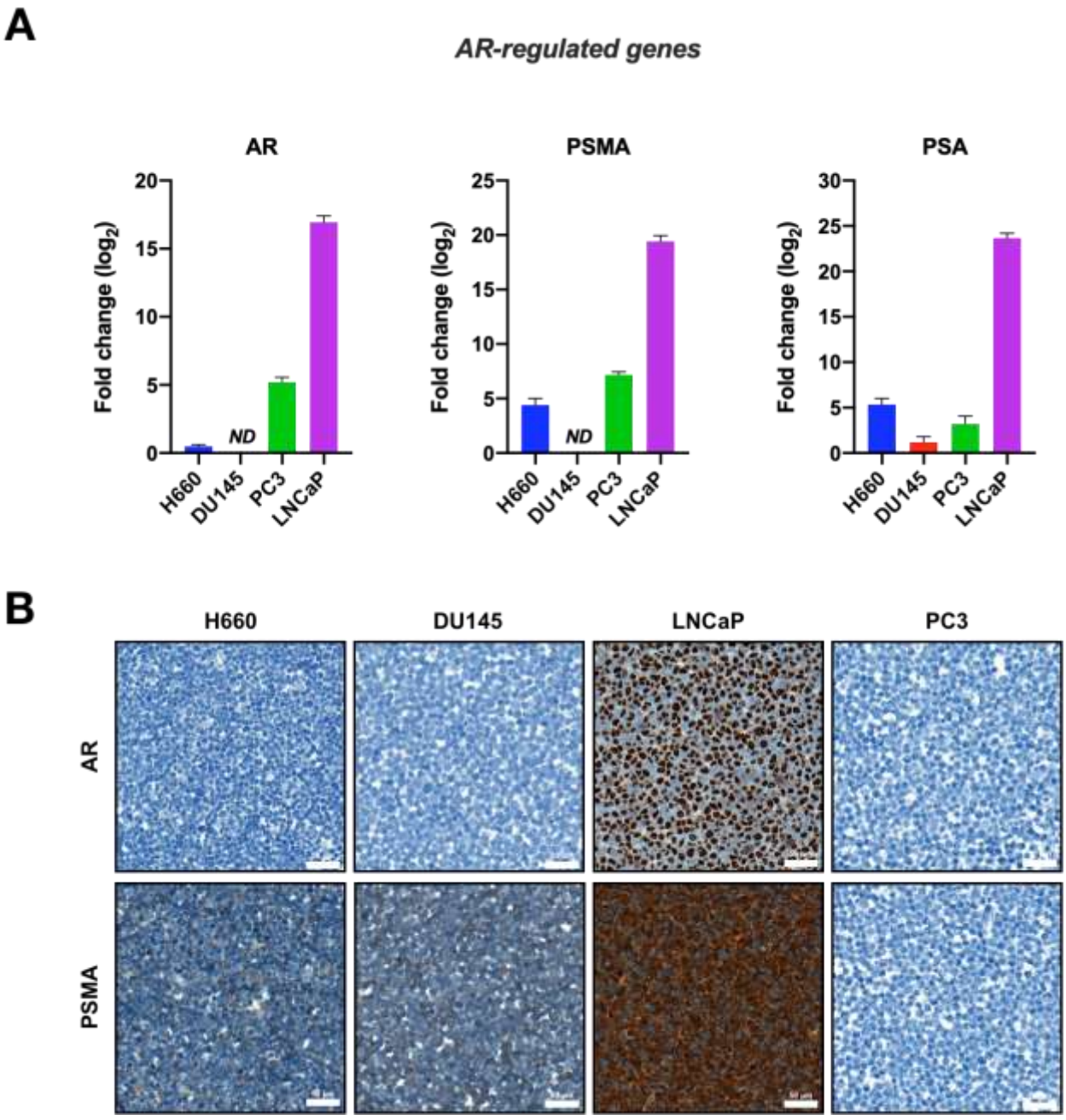

Supplemental Figure 1. AR, PSMA, and PSA are absent in H660 cells at the transcriptional and translational level. A. RT-PCR shows the expression patterns of the *AR* gene (*AR*), *PSMA* gene (*FOLH1*), and *PSA* gene (*KLK3*) in DU145, PC3, H660, and LNCaP cells compared to A549 (*PSMA* and *PSA*) and H82 (*AR*) negative controls (not shown). *ND*, not detected **B.** Representative immunohistochemistry images of H660 (AR-/PSMA-), DU145 (AR-/PSMA-),

LNCaP (AR+/PSMA+), and PC3 (AR-/PSMA-) tumor cell sections for AR and PSMA. Scale bars, 50 μm.

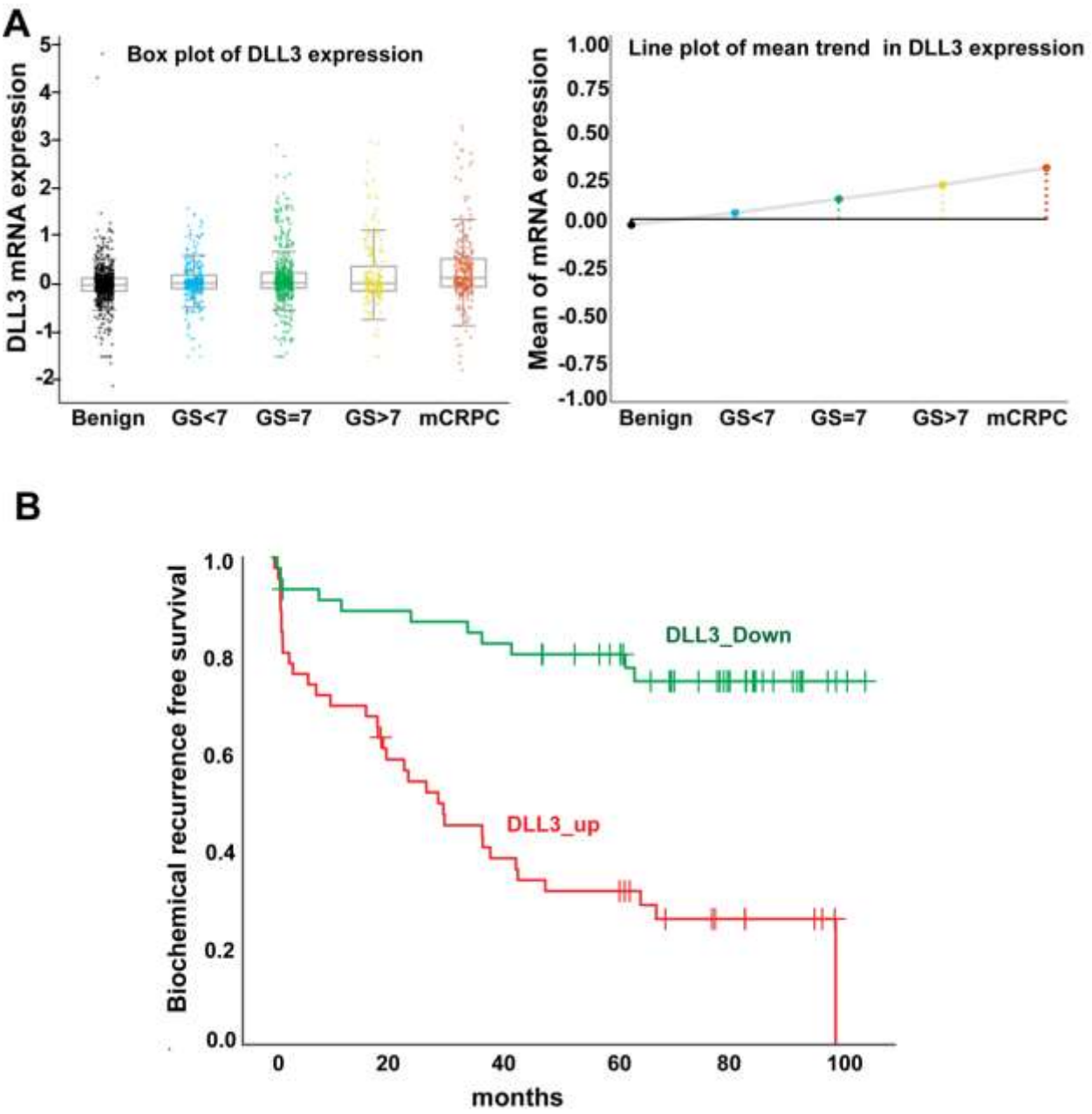

Supplemental Figure 2. Overexpression of *DLL3* associated with prostate cancer progression. A. The box plot showing the upregulation of *DLL3* mRNA expression in advanced prostate cancer (Left). The line plot showing the mean trend of *DLL3* mRNA expression in various grades and stages of prostate cancer (Right). The graphs were generated using Prostate Cancer Transcriptome Atlas and p-value between groups was determined by one way ANOVA. One-way ANOVA test between subsets: F-value = 14.030, P-value = <0.001; Ranksums-test

between subsets (mCRPC VS Primary): Fold change = 0.179, P-value = <0.001; Ranksums-test between subsets (Primary VS Benign): Fold change = 0.133, P-value = <0.001 **B.** Disease/progression-free survival (probability of freedom from biochemical recurrence) according to *DLL3* mRNA expression status among patients in the Ross-Adams *et al*. prostate cancer cohort (GSE70769). Log-rank test was used to compare groups. Survival curve and cox potential hazard regression analysis were performed using Prostate Cancer Transcriptome Atlas.

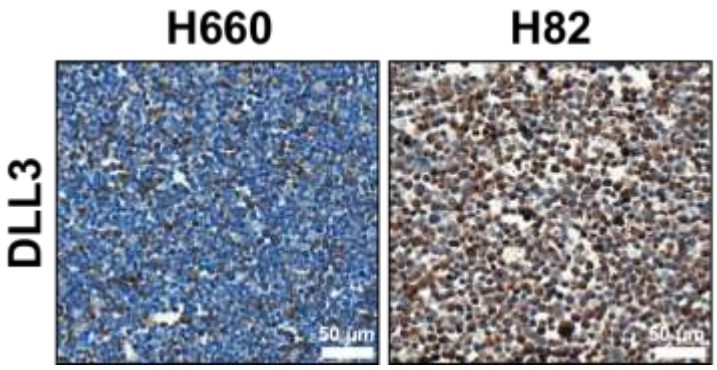

Supplemental Figure 3. Representative immunohistochemistry images of H660 and H82 tumor cell sections for DLL3. Scale bars, 50 µm.

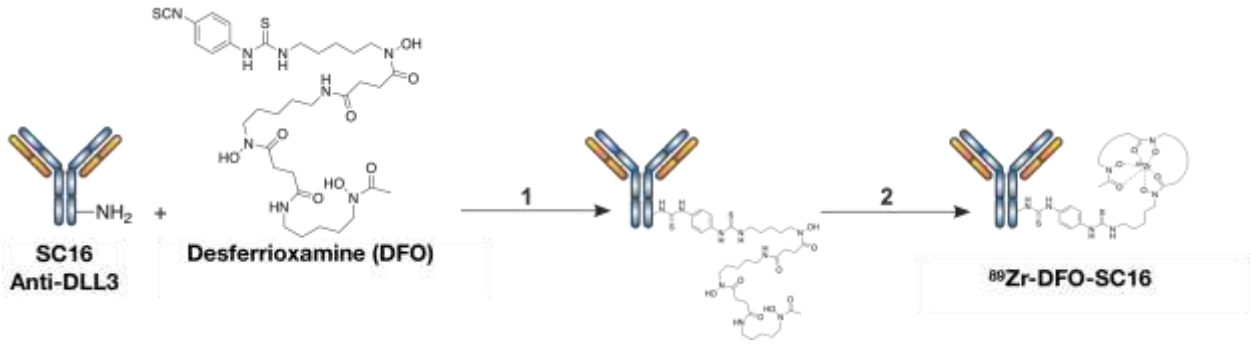

Supplemental Figure 4. Overview of the synthesis of ^{89}Zr-DFO-SC16. Schematic representation of ^{89}Zr-DFO-SC16 preparation showing DFO conjugation to SC16 and then radiolabeling of the DFO-SC16 construct. (1) PBS/Na_2CO_3, pH 9.0, 37 ºC, 90 min; (2) ^{89}Zr-oxalate, pH 6.8; PBS, RT, 1h.

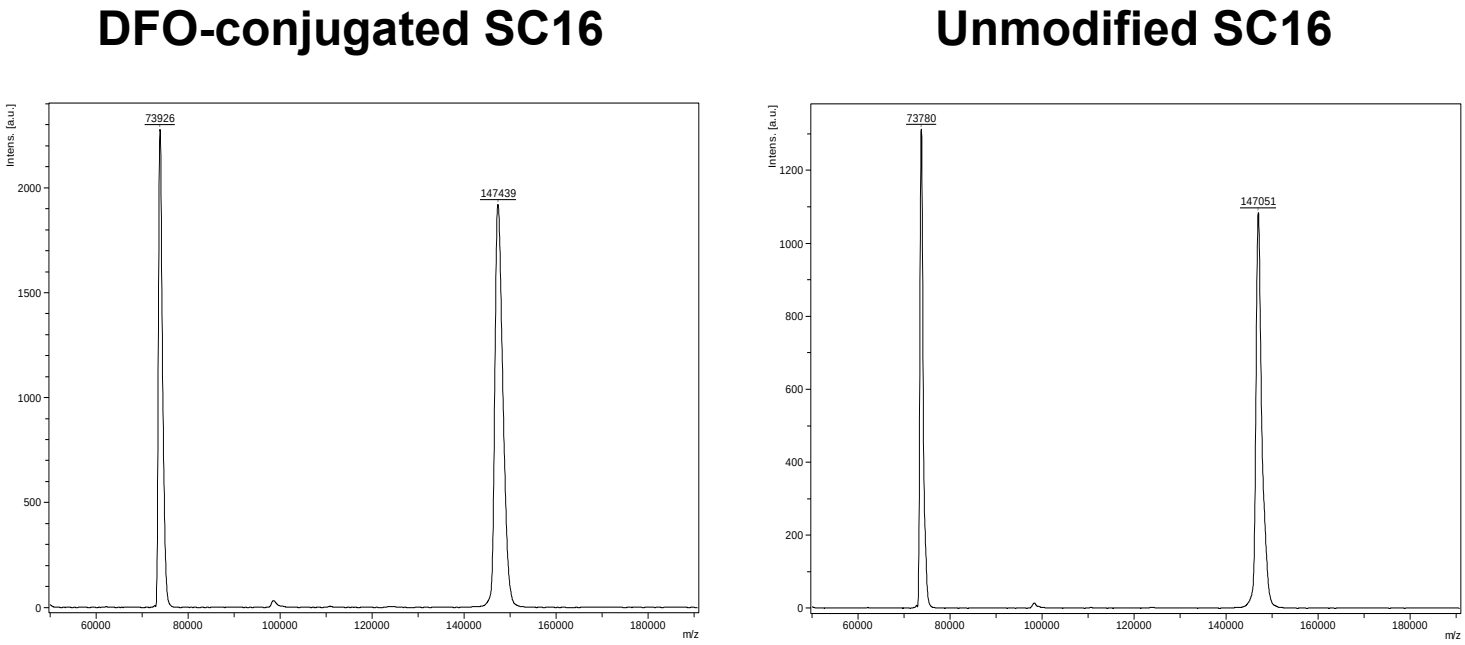

Supplemental Figure 5. MALDI-TOF spectra of the unmodified SC16 and the DFO-conjugated SC16. Representative spectra show a peak corresponding to the mass of the unmodified SC16 antibody (MW ~ 147051) and peak corresponding to the DFO-conjugated SC16 antibody (MW ~147439). Analysis revealed an average of 0.44 DFOs conjugated to SC16.

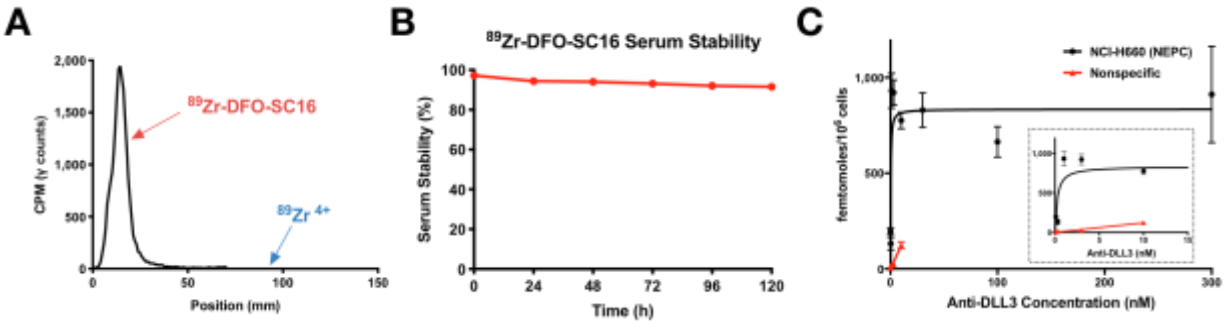

Supplemental Figure 6. A. Radio-iTLC of ^{89}Zr-DFO-SC16 after purification by PD-10 column. High radiochemical purity (> 99%) was achieved. **B.** The purified ^{89}Zr-DFO-SC16 was incubated in human serum at 37 ºC. Stability of the construct, as determined by radio-iTLC, was shown to be > 92% stable over a 5-day period. **C.** A plot of the saturation binding curve of ^{89}Zr-DFO-SC16 to H660 cells. Data analysis performed using PRISM revealed values for B_{max} = 862.6 ± 55.5 femtomoles/10^6 cells and K_d < 1 nM.

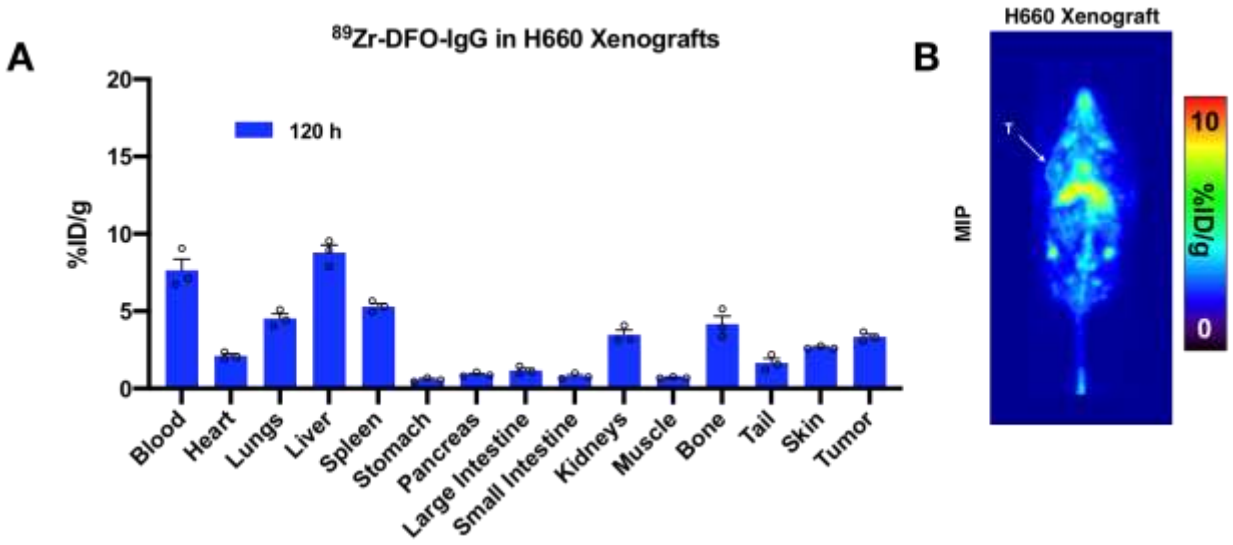

C

Time	120 h (n = 3)
	%ID/g ± SEM
Blood	7.64 ± 0.72
Heart	2.10 ± 0.14
Lungs	4.52 ± 0.30
Liver	8.79 ± 0.49
Spleen	5.30 ± 0.20
Stomach	0.56 ± 0.07
Pancreas	0.91 ± 0.07
Large Intestine	1.16 ± 0.14
Small Intestine	0.79 ± 0.10
Kidneys	3.47 ± 0.30
Muscle	0.71 ± 0.02
Bone	4.16 ± 0.52
Tail	1.66 ± 0.28
Skin	2.65 ± 0.06
Tumor	3.34 ± 0.17

Supplemental Figure 7. Full biodistribution data and imaging of ^{89}Zr-DFO-IgG after lateral tail vein injection in H660 subcutaneous xenograft bearing mice. **A.** Percent injected dose per gram of tissue after five days. **B.** Maximum intensity projection (MIP) of ^{89}Zr-DFO-IgG in male nude mouse xenografted with H660 tumor on the left shoulder. **C.** Tabulated biodistribution data expressed as mean %ID/g ± SEM.

A

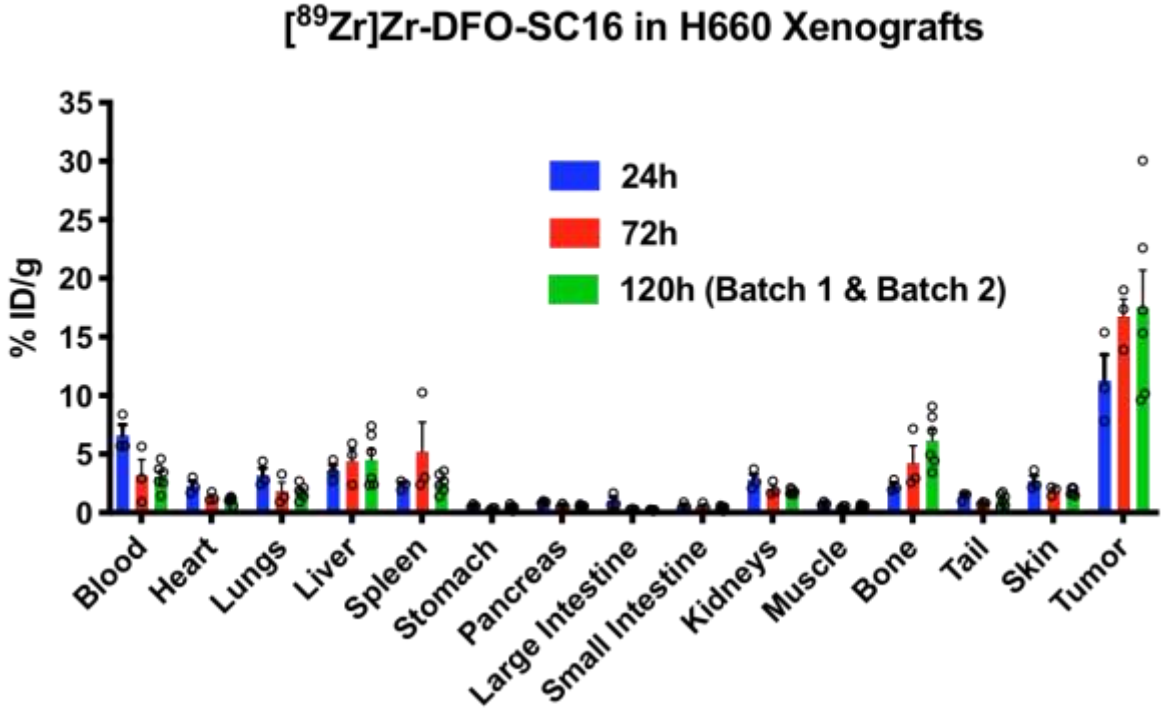

B

Time	24 h (n = 3)	72 h (n = 3)	120 h (n = 6)
	%ID/g ± SEM	%ID/g ± SEM	%ID/g ± SEM
Blood	6.60 ± 0.90	3.16 ± 1.37	3.07 ± 0.45
Heart	2.30 ± 0.39	1.35 ± 0.21	1.08 ± 0.11
Lungs	3.19 ± 0.61	1.84 ± 0.73	1.78 ± 0.25
Liver	3.58 ± 0.50	4.40 ± 1.05	4.50 ± 0.91
Spleen	2.36 ± 0.22	5.20 ± 2.53	2.55 ± 0.33
Stomach	0.60 ± 0.08	0.35 ± 0.04	0.45 ± 0.08
Pancreas	0.90 ± 0.07	0.59 ± 0.09	0.55 ± 0.05
Large Intestine	1.03 ± 0.33	0.30 ± 0.02	0.23 ± 0.02
Small Intestine	0.58 ± 0.16	0.53 ± 0.17	0.39 ± 0.07
Kidneys	2.81 ± 0.48	2.05 ± 0.32	1.78 ± 0.09
Muscle	0.78 ± 0.08	0.51 ± 0.06	0.54 ± 0.06
Bone	2.29 ± 0.26	4.23 ± 1.47	6.17 ± 0.91
Tail	1.37 ± 0.20	0.82 ± 0.06	1.12 ± 0.21
Skin	2.70 ± 0.46	1.87 ± 0.22	1.83 ± 0.13
Tumor	11.28 ± 2.21	16.75 ± 1.51	17.50 ± 3.19

Supplemental Figure 8. Full biodistribution data of ^{89}Zr-DFO-SC16 after lateral tail vein injection in H660 subcutaneous xenograft bearing mice. **A.** Percent injected dose per gram of tissue over five days. **B.** Tabulated biodistribution data expressed as mean %ID/g ± SEM.

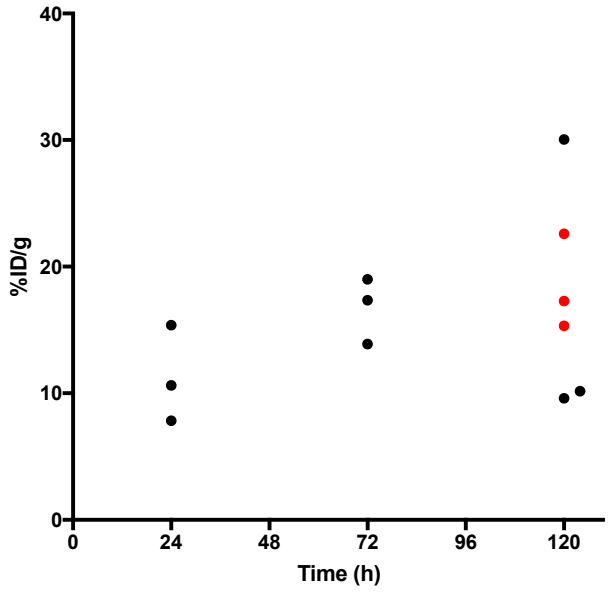

Supplemental Figure 9. ^{89}Zr-DFO-SC16 accumulation at the tumor site increases overtime. Antibody-tumor accumulation at 24, 72, and 120 h post-intravenous injection of ^{89}Zr-DFO-SC16 in athymic nude mice bearing subcutaneous H660 tumors. Data points in black color represent data obtained from batch #1 containing n = 3 mice per group. Because the data obtained at 120 h was slightly different among the 3 mice, we repeated the study for this time-point using batch #2 containing another n = 3 mice per group. Mice from batch #2 were also used for imaging studies shown in Figures 4A and supplemental figure 3. Statistical analyses were performed using Rstudio to account for batch effects determining a correlation between X (time after antibody administration) and Y (%ID/g) and accounting for the extraneous variable Z (mice cohort). Regardless of having data obtained from 2 different mice cohorts, we observed a positive correlation (as determined by linear regression analyses) between X and Y (P = 0.00971).

A

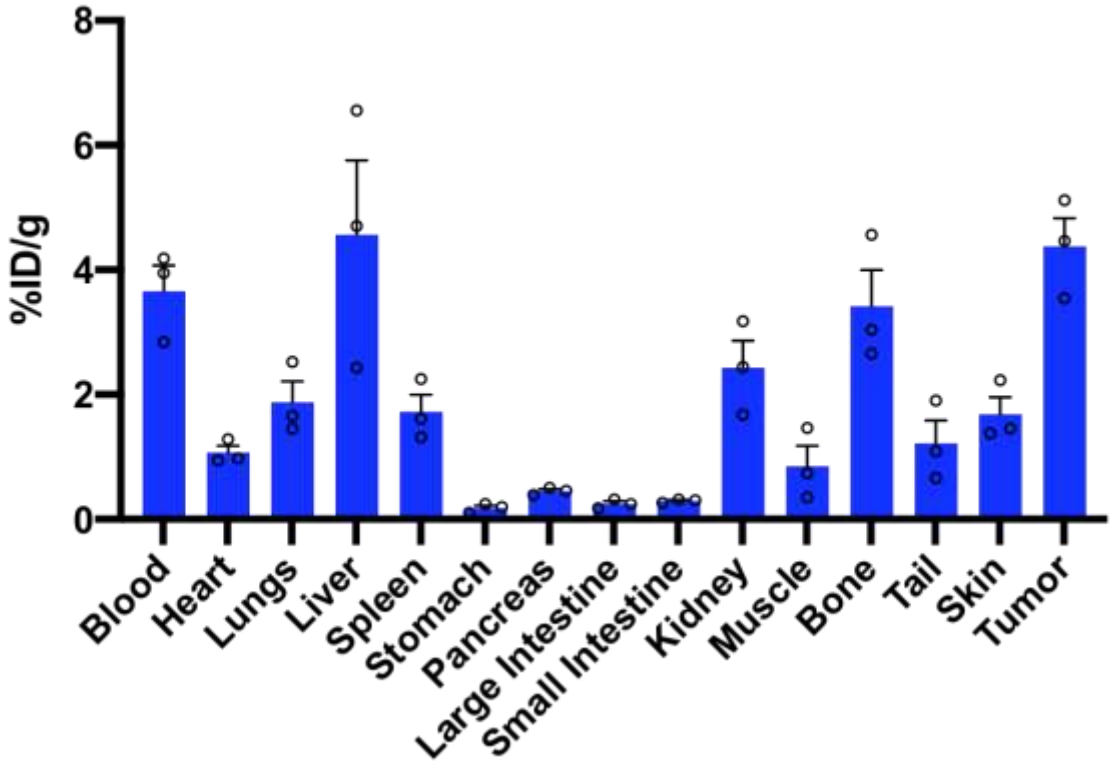

B

Time	72 h Block (n = 3)
	%ID/g ± SEM
Blood	2.63 ± 0.71
Heart	0.79 ± 0.14
Lungs	1.31 ± 0.26
Liver	2.85 ± 0.33
Spleen	1.23 ± 0.14
Stomach	0.14 ± 0.05
Pancreas	0.36 ± 0.02
Large Intestine	0.16 ± 0.02
Small Intestine	0.18 ± 0.03
Kidneys	1.62 ± 0.15
Muscle	0.58 ± 0.16
Bone	2.55 ± 0.46
Tail	0.78 ± 0.15
Skin	1.20 ± 0.17
Tumor	3.01 ± 0.36

Supplemental Figure 10. Full biodistribution data of ^{89}Zr-DFO-SC16 with a 50-fold excess of

cold, unlabeled SC16 antibody after lateral tail vein injection in H660 subcutaneous xenograft bearing mice. **A.** Percent injected dose per gram of tissue 72 h post-injection. **B.** Tabulated biodistribution data expressed as mean %ID/g ± SEM.

A

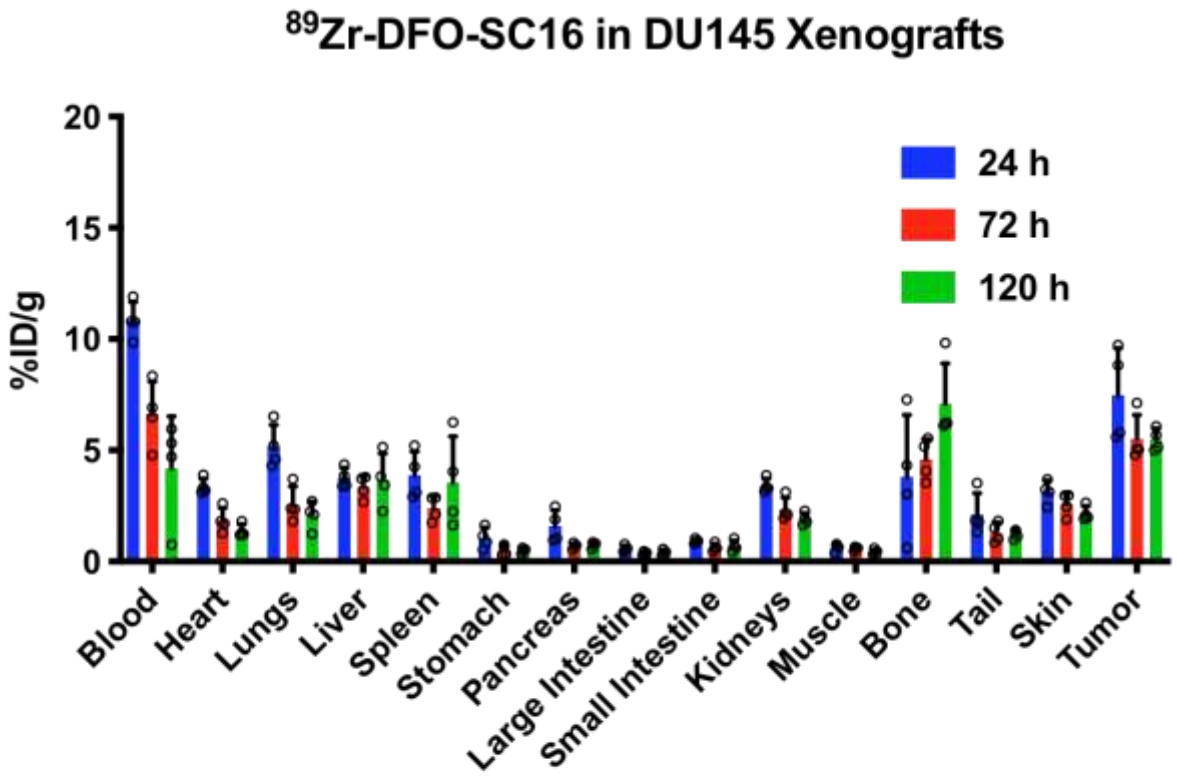

B

Time	24 h (n = 4)	72 h (n = 4)	120 h (n = 4)
	%ID/g ± SEM	%ID/g ± SEM	%ID/g ± SEM
Blood	10.84 ± 0.42	6.63 ± 0.73	4.19 ± 1.17
Heart	3.38 ± 0.18	1.85 ± 0.28	1.38 ± 0.14
Lungs	5.16 ± 0.49	2.56 ± 0.40	2.08 ± 0.31
Liver	3.76 ± 0.23	3.36 ± 0.26	3.67 ± 0.59
Spleen	3.87 ± 0.54	2.40 ± 0.28	3.55 ± 1.04
Stomach	1.05 ± 0.24	0.51 ± 0.11	0.49 ± 0.06
Pancreas	1.59 ± 0.36	0.69 ± 0.06	0.72 ± 0.07
Large Intestine	0.58 ± 0.07	0.37 ± 0.04	0.39 ± 0.06
Small Intestine	0.91 ± 0.05	0.63 ± 0.09	0.69 ± 0.13
Kidneys	3.41 ± 0.16	2.33 ± 0.27	1.92 ± 0.13
Muscle	0.63 ± 0.09	0.57 ± 0.04	0.44 ± 0.06
Bone	3.81 ± 1.39	4.58 ± 0.47	7.10 ± 0.91
Tail	2.12 ± 0.48	1.30 ± 0.23	1.22 ± 0.10
Skin	3.12 ± 0.26	2.58 ± 0.25	2.16 ± 0.16
Tumor	7.48 ± 1.05	5.50 ± 0.54	5.47 ± 0.25

Supplemental Figure 11. Full biodistribution data of ^{89}Zr-DFO-SC16 after lateral tail vein injection in DU145 subcutaneous xenograft bearing mice. **A.** Percent injected dose per gram of tissue over five days. **B.** Tabulated biodistribution data expressed as mean %ID/g ± SEM.

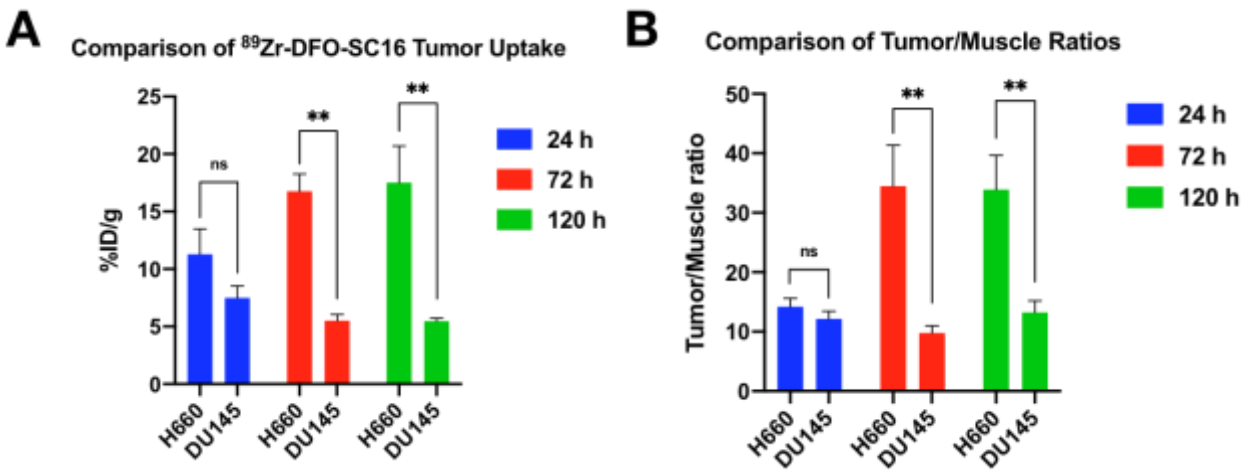

Supplemental Figure 12. DLL3 is specific and selective for DLL3-expressing H660 tumors. **A.** Biodistribution of ^{89}Zr-DFO-SC16 after lateral tail vein injection in H660 xenograft bearing mice and DU145 xenograft bearing mice. The tumoral uptake increases over time in the H660 xenograft. Contrarily, tumor uptake remains relatively constant over the same time frame in the DU145 xenograft. %ID g^{-1}, percentage of injected dose per gram. $^{**}p < 0.01$. **B.** Tumor-to-muscle ratio comparisons over time from the uptake of ^{89}Zr-DFO-S16 in H660 and DU145 xenograft bearing mice. $^{**}p < 0.01$.

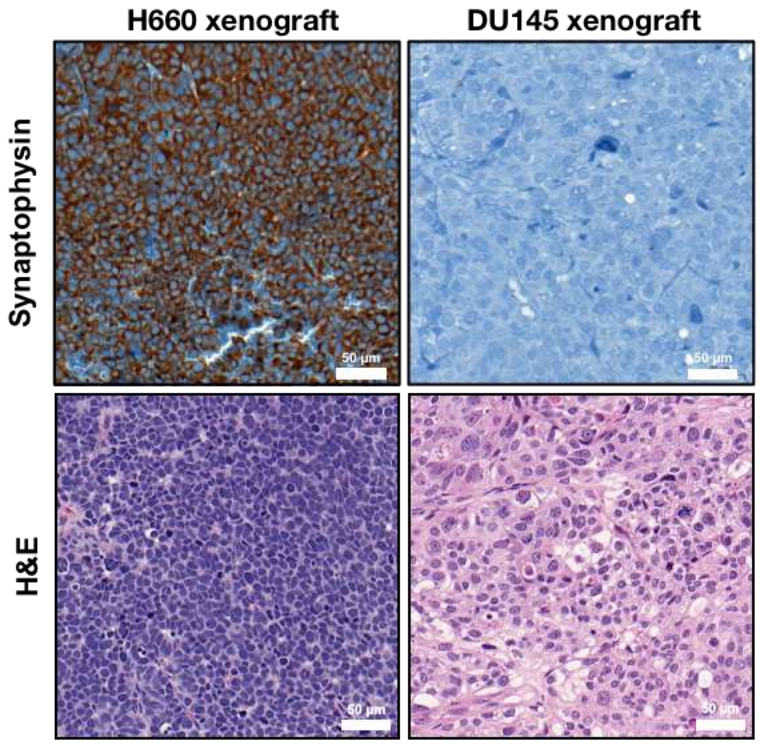

Supplemental Figure 13. Representative immunohistochemistry of H660 and DU145 subcutaneous tumor xenografts for SYP. Additionally, representative H&E images are shown. Scale bars, 50 µm.

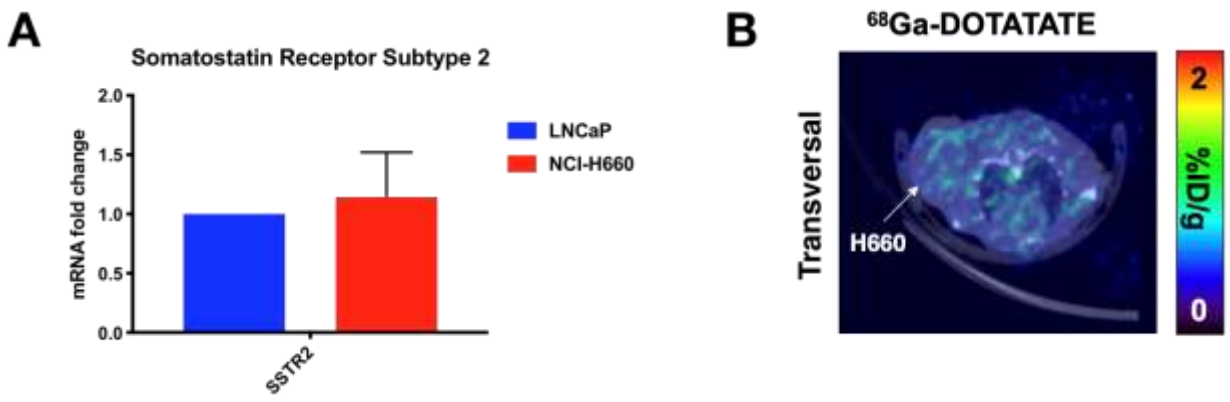

Supplemental Figure 14. ^{68}Ga-DOTATATE cannot image NEPC lesions *in vivo*. A. RT-PCR shows the expression pattern of the SSTR2 gene in H660 as compared to LNCaP cells. No expression of the SSTR2 gene is observed in H660 cells. **B.** PET image of ^{68}Ga-DOTATATE (1h post-injection) in an athymic nude male mouse bearing subcutaneous H660 tumor. Representative transverse planar image is shown.